Nuclear Factor-κB Inhibition by Parthenolide Potentiates the Efficacy of Taxol in Non–Small Cell Lung Cancer *In vitro* and *In vivo*

Dianliang Zhang,[1,2] Lin Qiu,[1] Xianqing Jin,[1] Zhenhua Guo,[1] and Chunbao Guo[1]

[1]*Laboratory of Surgery, Children's Hospital of Chongqing Medical University, Chongqing, P.R. China and* [2]*Department of Surgery, Affiliated Hospital of Qingdao University, Qingdao, P.R. China*

Abstract

In this study, we have examined the molecular events induced by parthenolide, a sesquiterpene lactone, and explored possible mechanisms of resistance and sensitization of tumor cells to Taxol. We showed that parthenolide could antagonize Taxol-mediated nuclear factor-κB (NF-κB) nuclear translocation and activation and Bcl-xl up-regulation by selectively targeting I-κB kinase activity. In A549 cells, inhibition of nuclear factor-κB by parthenolide resulted in activation of the mitochondrial death pathway to promote cytochrome *c* release and caspase 3 and 9 activation. In contrast, Taxol alone induced apoptosis via a pathway independent of mitochondria cytochrome *c* cascade. In addition, depletion of Bcl-xl rescued the apoptotic response to Taxol. Moreover, treatment with parthenolide increased the efficacy of the Taxol-induced inhibition of A549 tumor xenografts in mice. This study elucidated the cellular responses induced by parthenolide that decrease the threshold of mitochodria-dependent apoptosis in the treatment of non–small cell lung cancer cells. (Mol Cancer Res 2009;7(7):1139–49)

Introduction

Taxol, an antimicrotubule agent, has significant antitumor activity against lung cancer. Nevertheless, most of patients with advanced lung cancer are destined to develop resistance to Taxol (1, 2). Although the molecular basis of resistance to Taxol is not well-documented, mounting evidence supports the role of intrinsically or constitutively activated nuclear factor-κB (NF-κB) in affording protection against programmed cell death. Constitutive high levels of NF-κB activity have been detected in response to chemotherapy and radiation in ovarian cancer (3-5), pancreatic cancer (6), breast cancer (7, 8), and prostate cancer (9). Our recent work has revealed that nuclear RelA and cytoplasmic pI-κBα are significantly associated with a poor prognosis in cancer (10). Furthermore, chemotherapy- induced activation of NF-κB can blunt the ability of the chemotherapy itself to induce cell death in lung cancer cells (11, 12). NF-κB is involved in the regulation of transcription of various genes involved in cell proliferation, angiogenesis, metastasis, and apoptosis (13, 14), which seems to lie at the heart of the ability of NF-κB to promote cancer therapy resistance. Therefore, inhibition of NF-κB may be an effective treatment strategy for many cancers resistance to chemotherapy. Many researchers have focused their efforts on exploring drugs with NF-κB suppression activity to directly kill cancer cells or render them more vulnerable to chemotherapeutic agents (15-17). Currently, several agents that can inhibit NF-κB function might be considered as an adjuvant approach in combination with Taxol for lung cancer (8, 18-21). Moreover, using drug combinations with nonoverlapping toxicity profiles and decreasing doses of individual agents may reduce the severity of undesired side effects of chemotherapy.

In resting cells, NF-κB proteins are normally sequestered in the cytoplasm in an inactive state in a complex with inhibitor I-κB. Stimulus-mediated degradation of I-κB by phosphorylation via I-κB kinase (IKK) can release NF-κB; this allows it to translocate into the nucleus and bind DNA to activate transcription of responsive genes, which could mediate its biological activity. IKK therefore represents a major regulator of the NF-κB pathway, and because of the central role of NF-κB activity in important cellular functions, inhibitors of IKK show promise for the treatment of different human diseases. IKK is a complex composed of at least three different protein kinases, IKKα, IKKβ, and IKKγ. Both IKKα and IKKβ are highly similar catalytic subunits that are brought together through interactions with the regulatory subunit IKKγ. Previous biochemical and genetic analyses have shown that the IKKβ subunit of IKK plays the major role in cytokine-dependent activation of the IKK complex, so it is essential for NF-κB activation and prevention of apoptosis.

The active compound of feverfew (*Chrysanthemum parthenium*) parthenolide has shown potential significant cancer suppression activity *in vitro* and *in vivo* (22, 23). Several studies have proposed that parthenolide inhibits NF-κB DNA binding activity and function and thereby increases the sensitivity of breast cancer cells to the chemotherapeutic agent Taxol (24). Although the effect of parthenolide as an inhibitor of NF-κB activity has been reported previously in several cancer cell lines (22, 23, 25, 26), its significance, detailed mechanism, potential

Received 9/4/08; revised 3/3/09; accepted 4/1/09; published OnlineFirst 7/7/09.
Grant support: Key project of National Natural Science Foundation of China (NO. 30330590), National Natural Science Foundation of China (No: 30770950), and the key project of Chongqing Natural Science Foundation (CSTC, 2008BA0021).
The costs of publication of this article were defrayed in part by the payment of page charges. This article must therefore be hereby marked *advertisement* in accordance with 18 U.S.C. Section 1734 solely to indicate this fact.
Note: L. Qiu and D. Zhang contributed equally to this work.
Requests for reprints:]Chunbao Guo, Laboratory of Surgery, Children's Hospital of Chongqing Medical University, 136 Zhongshan 2nd Road Chongqing, 400014, P.R. China. Phone: 86-23-63893006; Fax: 86-23-63633006. E-mail: gchunbao@yahoo.com.cn

doi:10.1158/1541-7786.MCR-08-0410

use in treatment, and adjuvant approach in combination with Taxol chemotherapy has not yet fully been investigated in human non–small cell lung cancer (NSCLC).

To determine whether inhibition of the NF-κB pathway by parthenolide could sensitize lung cancer cells to Taxol inhibition, we evaluated the effectiveness of parthenolide in combination with Taxol *in vitro* and *in vivo*. The combination suppressed lung cancer cell growth and induced apoptosis to a greater degree than either agent alone. Joint targeting of the NF-κB pathway by parthenolide and Taxol simultaneously induced the mitochondria-dependent death pathway and the caspase-independent death pathway, respectively, resulting in a synergistic cytotoxicity. To our knowledge, the present study represents the first time the combined molecular and functional analysis of NF-κB and its related molecules.

Results

Potentiation of Taxol-Induced Apoptosis by Parthenolide In Vitro

To determine the effect of parthenolide, the active compound in feverfew, on cancer cell proliferation, human lung cancer cell lines A549, NCI-H446, and A549-T24 (resistant to Taxol treatment) were treated with increasing concentrations of parthenolide (1, 3, 5, 10, 15 μmol/L) for 24 hours. Parthenolide inhibited growth in a dose-dependent manner in all three cell lines. Significant growth inhibition was observed between 10 and 15 μmol/L parthenolide. At a concentration of 5 μmol/L, parthenolide did not significantly inhibit growth of the A549, A549-T24, and NCI-H446 cell lines after 24 hours of treatment (Fig. 1A). In addition, to confirm their sensitization to Taxol-induced cell suppression, we further did cell viability analysis in A549, NCI-H446, and A549-T24 cell lines incubated with parthenolide plus Taxol. As seen in Fig. 1B, Taxol treatment alone resulted in a concentration-dependent increase in growth inhibition by 20%. Cotreatment with parthenolide (5 μmol/L) plus Taxol further enhanced the inhibitory effects of Taxol on cell viability for A549 cells by 20% and NCI-H446 cells by almost 30% (Fig. 1B). This suggests that parthenolide at a concentration of 5 μmol/L does not trigger apoptosis alone, but could sensitize the cells' response to Taxol. A549 and NCI-H446 cells were the most sensitive to parthenolide and A549-T24 cells were least sensitive to parthenolide (Fig. 1B). The inhibitory effect of parthenolide and Taxol was more than that of BAY 11-7082 and Taxol (Fig. 1B). At a concentration of 5 μmol/L, BAY 11-7082 had no significant inhibitory growth effects as indicated previously (5). Similarly, the DNA fragmentation assay showed that cell death induced by Taxol and parthenolide occurred via the activation of an apoptotic program (data not shown).

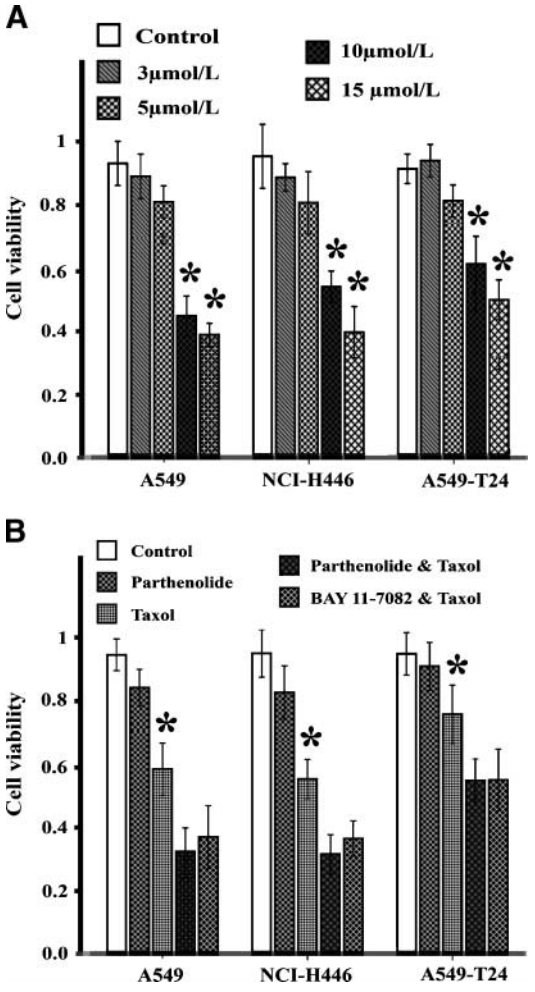

FIGURE 1. Parthenolide-potentiated inhibition of Taxol-induced cell growth. **A.** Inhibition of cell viability during a dose course with the concentrations of parthenolide indicated above, when incubated with A549 (*left*), NCI-H446 (*middle*), and A549-T24 (*right*) cells for 24 h. Cell viability was assessed by (4,5-dimethylthiazol-2-yl)2,5-diphenyl-tetrazolium bromide assay as described in Materials and Methods. $P < 0.01$, versus control group. **B.** A549 cells were alternatively pretreated with either 5 μmol/L parthenolide or BAY 11-7085, then incubated with 100 nmol/L Taxol for 24 h, as indicated above, when cell viability was assessed. Significant differences between the parthenolide-treated and not treated are indicated by asterisks. *, $P < 0.01$, versus parthenolide and Taxol group. The results represent average values from three independent experiments.

IKK Kinase Complex Mediates Taxol-Induced NF-κB Activation in Human NSCLC Cell Lines

NF-κB had been implicated in the resistance of human breast tumors, ovarian tumors, and epidermoid tumors to Taxol-induced apoptosis. To determine the possible effects that Taxol may have on NF-κB activity in human NSCLC cell lines, we compared NF-κB DNA-binding activities among human lung cancer cell lines A549, NCI-H446, and A549-T24 (resistant to Taxol treatment) treated with Taxol. As shown in Fig. 1, the basal level of NF-κB in A549-T24 cells was higher than that in A549 and NCI-H446 cells. NF-κB activity in A549 and NCI-H446 cells increased when exposed to 100 nmol/L Taxol for 24 h compared with the basal level (Fig. 2A). The differential response to Taxol was correlated with the level of basal NF-κB DNA-binding activity as measured by electrophoretic mobility shift assay (EMSA; Fig. 2A). Consistent with NF-κB DNA-binding activity as shown, Taxol transiently decreased the amount of phosphorylated I-κBα in A549 and NCI-H446 cells, whereas the total I-κBα was maintained at the resting level, suggesting that Taxol has no effect on the degradation of I-κBα (Fig. 2A). Thus, the more resistant A549-T24 cells exhibited higher levels of active NF-κB than the more responsive A549 and NCI-H446 cells. Previous studies have shown that phosphorylation of I-κBα is primarily

mediated by activation of IKK complex (17). To determine the involvement of endogenous IKK in response to Taxol-mediated I-κBα phosphorylation and NF-κB activation, phospho-IKKα/β was detected by immunoblotting, which showed that phosphorylated (active) IKK increased 24 hours after exposure to Taxol, consistent with the changes of NF-κB and I-kB induced by Taxol (Fig. 2A).

Next, we tested whether the inhibition of IKK using an IKK inhibitor (BAY 11-7082) was sufficient to block Taxol-induced NF-κB activation. Our results showed that IKK activity (as indicated by phospho-IKKα/β) was induced by Taxol in the human NSCLC cells lines and could be inhibited by BAY 11-7082, whereas the levels of IKK proteins (indicated as IKK-β) remained the same. We also found that Taxol-induced NF-κB activity, as measured by EMSA, was abrogated with BAY 11-7082 (Fig. 2B).

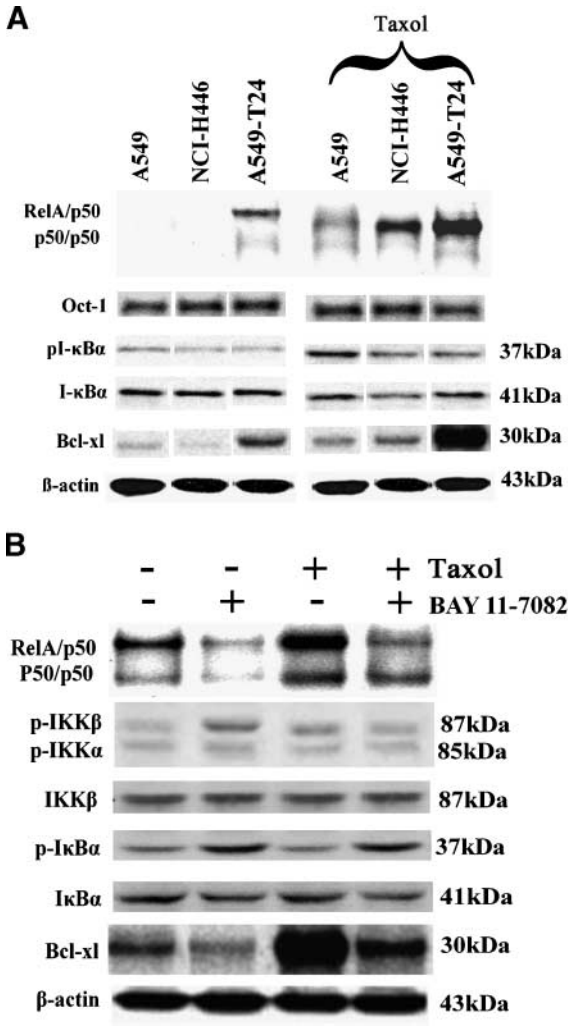

FIGURE 2. Effect of Taxol on NF-κB activation in A549, NCI-H446, and A549-T24 cell lines. **A.** The three cell lines were exposed to 100 nmol/L Taxol for 24 h. Nuclear extracts were prepared and examined for NF-κB DNA binding activities (RelA/p50) by EMSA. Oct-1 was selected as a constitutively expressed control. NF-κB activation related molecules, such as pI-κB, I-κB, and Bcl-xl (cytoplasmic extracts), were subjected to Western blotting with β-actin as the loading control. Representative figures of multiple experiments are shown. The positions of the molecular weight markers are noted on the right. **B.** BAY 11-7082 mediated inhibition of NF-κB induced by Taxol through IKK. A549 cells with or without pretreatment of 5 μmol/L BAY 11-7082 were treated with 100 nmol/L Taxol for 24 h. NF-κB DNA binding activities in the nuclear extract and phospho-I-κBα, I-κBα, p-IKKα/β, IKKα, and Bcl-xl in a cytosolic extract were compared. The positions of molecular weight markers are noted on the right.

Parthenolide Inhibits Taxol-Mediated Activation of IKK in the A549 Cell Line

Previous studies have verified that parthenolide can inhibit activation of IKK in pancreatic and hepatocellular carcinoma cells lines (25, 27). Here, we examined whether parthenolide has the same effect in human NSCLC lines. As expected, parthenolide significantly inhibited the activation of IKK in the A549 cell line in a concentration-dependent manner. Incubation with 10 μmol/L parthenolide for 24 hours completely inhibited Taxol-induced activation of IKK activity (data not shown). Moreover, NF-κB DNA binding activity in nuclear extracts prepared from A549 cells stimulated with Taxol could be completely abolished by 10 μmol/L parthenolide, as measured by EMSA (data not shown). Activation of IKK correlated with degradation of I-κB with a similar kinetics in A549 cells, which was prevented by parthenolide incubation (Fig. 3A). The effect was similar or stronger with BAY 11-7082 (Fig. 3A). The effect was concentration dependent, and those concentrations that showed no effect on apoptosis also inhibited the DNA-binding activity of NF-κB (5 μmol/L). Consistent with the finding above, strong p65 translocation to the nucleus was observed in A549 cells stimulated with Taxol and was completely inhibited when cells were incubated with 5 μmol/L parthenolide before Taxol stimulation (Fig. 3B).

Although our results suggest that parthenolide potentiates Taxol-mediated apoptosis by inhibition of IKK/NF-κB signaling, it remains possible that parthenolide might sensitize cells to apoptosis by IKK-independent pathways. To discriminate between these possibilities, A549 cells lacking or overexpressing IKKβ were generated and incubated with parthenolide plus Taxol. As seen in Fig. 3C, as expected, siRNA-IKKβ could block the IKK/NF-κB signaling cascade as measured by the DNA binding activity of NF-κB. Blocking expression of IKKβ resulted in the enhancement of Taxol-mediated apoptosis (Fig. 3D). Interestingly, parthenolide incubation within this system did not further enhance Taxol-induced cell death (Fig. 3C), whereas cells overexpressing IKKβ showed significant Taxol resistance and reversed the activity of parthenolide, as indicated by a decrease in the DNA-binding activity of NF-κB. These results were further confirmed by a cell viability assay and show that parthenolide sensitizes cells to Taxol-mediated killing by attenuating Taxol-induced IKK activation (Fig. 3D).

Synergistic Effect Elicited by Taxol and Parthenolide Through Cytochrome c–Dependent and -Independent Pathways

It has been reported that mitochondria play a minor role in Taxol-induced cell death of the lung cancer cell line H460 (28, 29). To verify if the caspase-independent mechanism of Taxol can be extrapolated to other NSCLC cell lines, the role of mitochondria in mediating cell death in A549 cells exposed

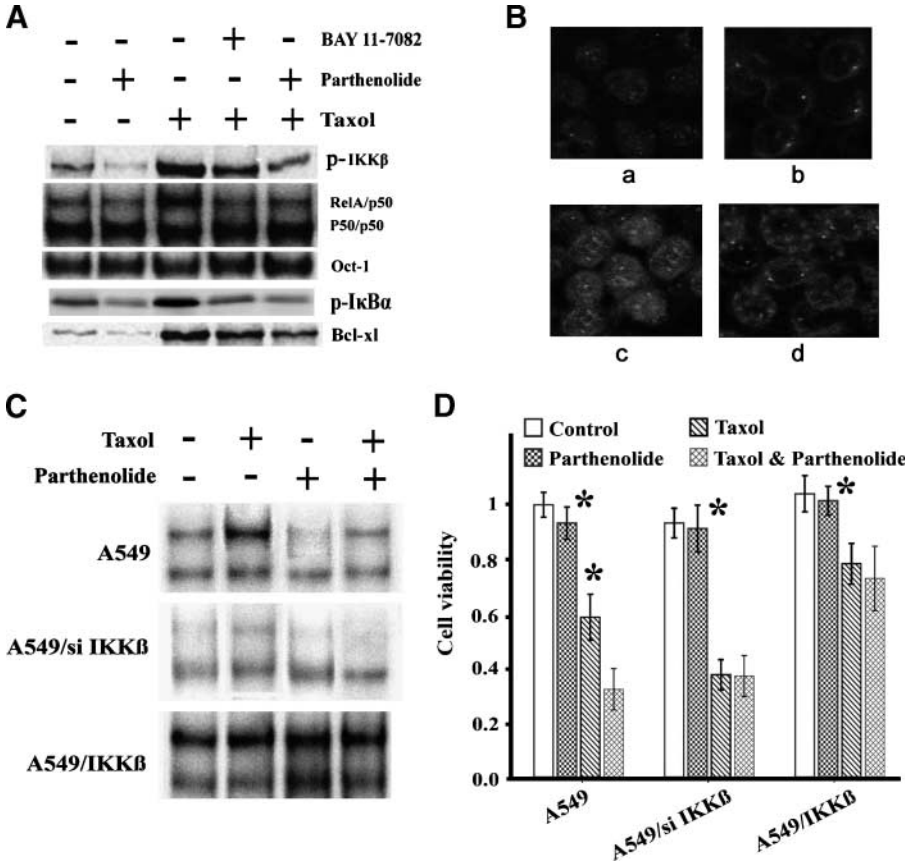

FIGURE 3. Regulation of NF-κB activation by parthenolide through IKK inhibition. **A.** A549 cells were alternatively pretreated with either 5 μmol/L parthenolide or 5 μmol/L BAY 11-7082 for 24 h and then incubated with Taxol for 24 h EMSA for the NF-κB binding and Western blot for p-IKKα/β and Bcl-xl were done **B.** Nuclear translocation of p65 was determined by indirect immunofluorescence. Representative fields show the exclusive cytoplasmic location of NF-κB in untreated control (**A**) and parthenolide-treated cells (**B**). Nuclear accumulation of p65 was indicated in Taxol-treated cells (**C**) and Taxol and parthenolide cells (**D**). **C.** A549 cells stably overexpressing Bcl-2 or depletion of Bcl-2 by transfection with siRNAs were generated as described in the Materials and Methods section. The A549 cells overexpressing or depleted of Bcl-2 or the empty vector control were treated with 5 μmol/L parthenolide and/or 100 nmol/L Taxol in succession, the cells were subjected to EMSA (NF-κB). **D.** Cell viability measurement for A549 cells overexpressing or silencing Bcl-2 and treated with 5 μmol/L parthenolide and/or 100 nmol/L Taxol in succession; columns, mean of three independent siRNA experiments; bars, confidence interval. *, significant differences $P < 0.01$ versus the same dose of Taxol plus parthenolide.

to Taxol was investigated by analyzing mitochondria stability, as determined by mitochondrial damage and the release of cytochrome *c*. We found that no decrease in mitotracker dye intensity, representing mitochondrial damage, could be detected after 24 hours of Taxol treatment (Fig. 4A). The A549 cells treated with Taxol only displayed a punctate staining pattern for cytochrome *c* (Fig. 4B). The release of cytochrome *c* from mitochondria in Taxol-treated A549 cells, which plays a key role in the apoptotic signal, could not be detected earlier than 48 h after treatment. These results suggest that Taxol is unable to activate the mitochondrial death pathway and trigger cell death in A549 cells.

Mitochondrial cytochrome *c* release due to NF-κB inhibition has been described previously (30). To additionally substantiate the role of parthenolide in response to the resistance to Taxol-induced apoptosis in A549 cells, we evaluated the chemosensitization effect of parthenolide in more detail by analyzing mitochondrial damage, cytochrome *c* release, and the caspase activity profile. Parthenolide-treated cells showed decreased intensity of mitochondrial dye (Fig. 4A) and mitochondrial damage, as evidenced by the release of cytochrome *c* into the cytoplasm. The punctate staining pattern of cytochrome *c* in A549 cells became diffuse after pretreatment parthenolide, indicating its release from mitochondria. This was further verified by the presence of cytochrome *c* in the cytoplasm (Fig. 4B). A concentration of 5 μmol/L of parthenolide was enough to induce cytochrome *c* release, which correlated with the concentration required to inhibit IKK and suggested a link between IKK inhibition and cytochrome *c* release.

We next assessed the activation of caspases 9 and 3 in the presence of parthenolide by immunoblotting. As indicated in Fig. 4C, parthenolide induced a marked increase in caspase activity that was not detected in A549 cells treated with Taxol. Pretreatment with zVAD-fmk could completely prevent the increase in caspase activity, even in the presence of Taxol. Thus, parthenolide can rescue the mitochondrial apoptotic response to Taxol in A549 cells, indicating that the simultaneous induction of the mitochondria-dependent death pathway by parthenolide and the caspase-independent death pathway by Taxol results in synergistic cytotoxicity.

Antiapoptotic Protein Bcl-xl Plays a Key Role in Resistance to Taxol-Induced Death

The mitochondria-associated antiapoptotic proteins, including different Bcl-2 family members and known NF-κB downstream target genes, were further investigated to determine the role of parthenolide in potentiating Taxol-induced cell death in A549 cells. Consistent with NF-κB DNA binding activity as shown, the antiapoptotic gene Bcl-xl was also up-regulated 24 hours after exposure to Taxol as indicated by the occurrence of Bcl-xl–specific bands with lower mobility in the gel (Fig. 5A). Taxol-induced Bcl-xl expression was suppressed by parthenolide (Fig. 5A). The inhibition of antiapoptotic molecules in A549 cells induced by parthenolide could also be

abolished with transfection with an IKKα or IKKβ siRNA, singly or in combination. These results indicate that parthenolide can also antagonize Taxol to diminish NF-κB–activated antiapoptotic molecule expression in A549 cells. To additionally examine the role of antiapoptotic Bcl-xl, A549 cells were transfected with Bcl-xl siRNA duplexes or control luciferase siRNA to silence Bcl-xl, and then treated with Taxol. Bcl-xl–depleted cells showed significant mitochondrial damage, as indicated by a decrease in the intensity of the mitochondrial dye.

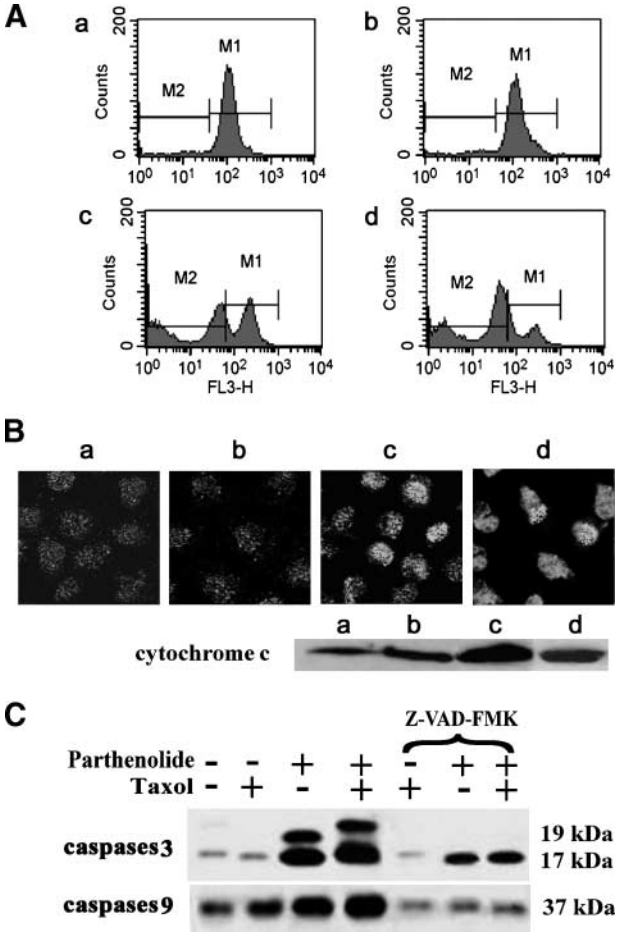

FIGURE 4. IKK inhibitor parthenolide induced mitochondrial membrane damage, mitochondrial cytochrome *c* release, and caspase activation in A549 cells. **A.** A549 cells were treated with 100 nmol/L Taxol and 5 μmol/L parthenolide singly or in combination for 24 h, after which cells were incubated with 100 nmol/L mitotracker red mitochondrial dye as described in Materials and Methods. The mitochondrial fluorescence intensity was analyzed by fluorescence-activated cell sorting. Representative fields were shown the strong intensity (*M1*) in untreated control (*a*), Taxol-treated cells (*b*), whereas cells with ruptured mitochondria showed decreased intensity (*M1*) in parthenolide-treated cells (*c*) and Taxol and parthenolide pretreated cells. **B.** A549 cells, treated with 100 nmol/L Taxol and 5 μmol/L parthenolide singly or in combination (*a*. Untreated control; *b*. Taxol-treated cells; *c*. Parthenolide-treated cells; and *d*. Taxol and parthenolide pretreated cells), were stained with monoclonal antibodies against cytochrome *c* and analyzed under a fluorescence microscopy confocal microscope (*top*). The cytosolic extract was prepared and subjected to Western blotting with a cytochrome *c* antibody (*bottom*). **C.** A549 cells were incubated with Z-VAD-fmk, subsequently incubated with 5 μmol/L parthenolide and/or 100 nmol/L Taxol. Cytosolic proteins were extracted, separated, and incubated with antibodies recognizing active caspases 3 and 9 as indicated.

Also, in Bcl-xl–depleted cells, parthenolide induced a marked decrease in the intensity of the mitochondrial dye, and this was not detected in Bcl-xl–depleted cells treated with Taxol (Fig. 5B).

Interestingly, in the absence of Bcl-xl, Taxol could not induce an increase in cytochrome *c* release, but could induce a marked increase in cell death that was not detected in control A549 cells treated with Taxol or in Bcl-xl–depleted cells without Taxol treatment (Fig. 5C and D). Parthenolide incubation within this system could slightly enhance cytochrome *c* release in Bcl-xl–depleted cells (Fig. 5C), suggesting that depletion of Bcl-xl can partly abolish the activity of parthenolide. Additionally, this indicates the functional activity of Bcl-xl in these cells. Moreover, the partial inhibitory effect of Bcl-xl on apoptosis is in line with the observed cytochrome *c* release in the parental cells (Fig. 5C and D). These results suggest that specific inhibition of NF-κB activity, which regulates expression of the antiapoptotic gene Bcl-xl, results in the induction of apoptosis.

Parthenolide Sensitizes Tumors to Taxol-Induced Cytotoxicity In Vivo

The *in vivo* antitumor activity of the Taxol/parthenolide combination was further evaluated in human A549 cell line xenografts in nude mice. To determine the optimum doses for parthenolide, human A549 xenograft-bearing nude mice were treated with parthenolide at different doses ranging from 1 to 50 mg/kg. At 25 mg/kg parthenolide, there was a significant inhibition of tumor growth, whereas there was no obvious antitumor activity at the dose of 20 mg/kg. Hence, we selected the dose of 20 mg/kg as the optimum dose for the combination treatment with Taxol. The Taxol doses used were of drug formulations and concentrations that would facilitate a single i.p. injection, and low drug concentrations of Taxol and parthenolide in combination were adopted.

As indicated in Fig. 6A, the mean tumor volume of the combination treatment group was significantly lower than either of the corresponding single treatment groups ($P < 0.05$, two-tailed Student's t test) after day 30. Combined treatment of Taxol (20 mg/kg) plus parthenolide showed a greater suppression of the tumor growth relative to Taxol alone, whereas parthenolide alone was unable to significantly inhibit tumor growth in the A549 xenograft–bearing mice (Fig. 6A). In the same manner, the combination of Taxol therapy with parthenolide also resulted in a significant increase in the life span (Fig. 6B) of the A549 xenograft mice. Moreover, the combination treatment was well-tolerated. No adverse consequences or potential toxicity were apparent by gross measures, such as weight loss, ruffling of fur, behavior, or feeding, in the combination treatment group, whereas a transient 10% body weight loss was noted in the Taxol group (data not shown). Analysis of peripheral blood revealed that treatment with parthenolide alone did not show a decrease in blood cells, no further significant decrease in blood cells was observed in the combined treatment group compared with the Taxol group (data not shown). Treatment with parthenolide or Taxol alone did not affect the apoptosis rate of tumor cells, whereas the density of the apoptotic cancer cells apparently increased after the combined therapy (Fig. 6C). We further confirmed whether NF-κB activities changed with parthenolide treatment *in vivo*. Subcellular localization of

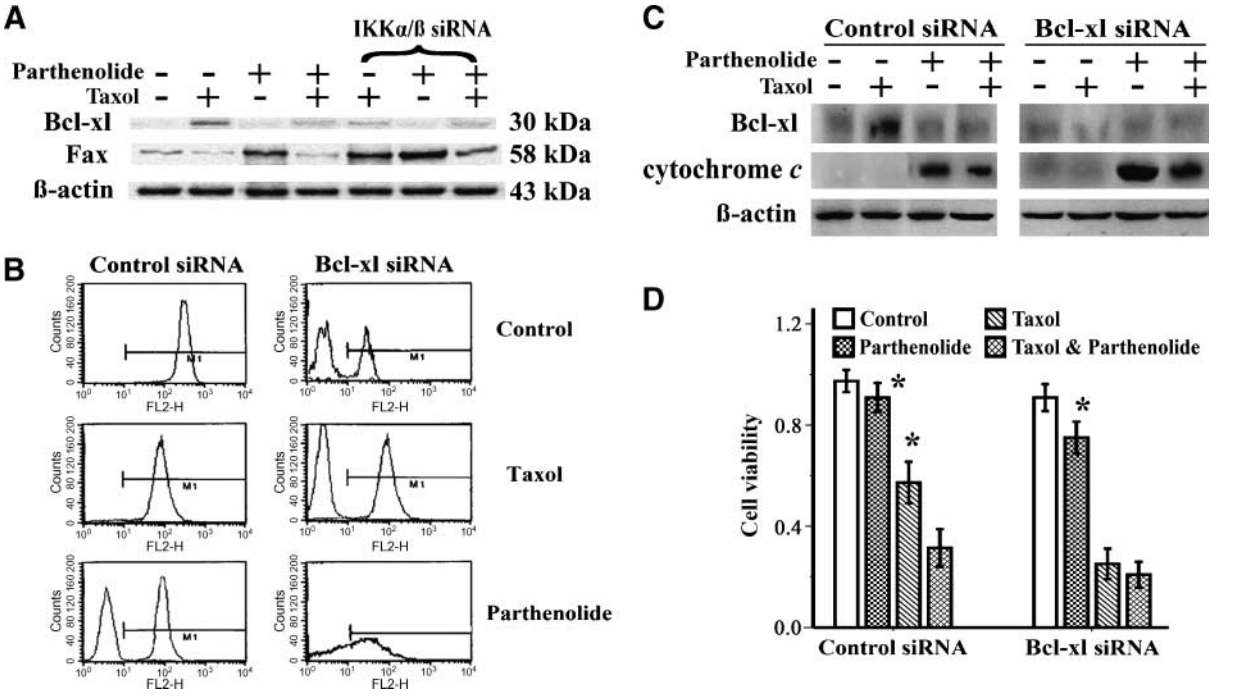

FIGURE 5. Depletion of Bcl-xl enhances Taxol-induced apoptosis in A549 cells. **A.** Influence of parthenolide on apoptosis-related gene expression. IKKβ siRNA and control scrambled siRNA-transfected A549 cells (data not shown) were treated with parthenolide (5 μmol/L) alone or in combination with Taxol (100 nmol/L) for 24 h. Equal amounts (50 μg/lane) of cytoplastic extracts were subjected to Western blotting by immunoblotting with antibodies against the various proteins as indicated. The positions of molecular weight markers are noted on the right. **B.** Bcl-xl depletion A549 cells by siRNA or its control were treated with parthenolide (5 μmol/L) alone or in combination with Taxol (100 nmol/L). The mitochondrial fluorescence intensity was analyzed by fluorescence-activated cell sorting as described above. **C.** Bcl-xl protein levels were analyzed by Western blot using anti–Bcl-xl antibody in Bcl-xl–depleted A549 cells or controls, which were treated with parthenolide (5 μmol/L) alone or in combination with Taxol (100 nmol/L); β-actin was probed as a loading control. **D.** Cell viability was assessed for Bcl-xl depleted A549 cells or controls, which were treated with parthenolide (5 μmol/L) alone or in combination with Taxol (100 nmol/L) as indicated in the Materials and Methods. Significant differences from the values between the treated with parthenolide group or not treated group are indicated by asterisks. *, $P < 0.01$, versus parthenolide and Taxol group. The results represent average values from three independent experiments.

RelA/NF-κB and phosphorylated I-κBα were assessed by immunohistochemistry. Figure 6D shows the representative pattern of increased RelA/NF-κB and phosphorylated I-κBα staining in both the cytoplasm and nuclei. The positive nuclear staining represents the active form. The cytoplasmic and nuclear staining rates of RelA/NF-κB were statistically lower in tumors treated with parthenolide compared with rates in tumors treated with vehicle alone. The prominent expression of phosphorylated I-κBα protein in the cytoplasm was also reduced in tumors treated with parthenolide compared with control tumors, suggesting that parthenolide inhibited the partial nuclear translocation of NF-κB p65 *in vivo*. Our data suggest that the traditional chemotherapeutic Taxol used in combination with parthenolide may be practical for NSCLC cancer treatment with less host toxicity and superior antitumor activity, for which patients usually receive adjuvant Taxol-based chemotherapy.

Discussion

Constitutive activation of NF-κB has been described in a great number of solid tumors, and this activation seems to support cancer cell survival and to reduce the sensitivity of cells to chemotherapeutic drugs. In this study, we used the inhibitory effect of parthenolide on Taxol-induced NF-κB to discover that NF-κB is up-regulated by Taxol at the clinically relevant concentration of 100 nmol/L in several Taxol-sensitive and resistance cell lines. Conversely, parthenolide (5 μmol/L) was found to possess an inverse regulatory effect on NF-κB that was mediated through IKK kinase complex. The inverse regulatory effects of Taxol and parthenolide on IKK implies that IKK might be an important mediator involved in the ability of parthenolide to potentiate Taxol-induced apoptosis. Further studies revealed that caspase activity is up-regulated when A549 cells are treated with lower concentrations of parthenolide (5 μmol/L), whereas mitochondrial stabilization is usually not detectable after Taxol treatment. This result implies that parthenolide-induced down-regulation of I-κBα may be dependent on mitochondrial stabilization. The synergistic effect of the combined use of Taxol and parthenolide may be influenced by both cascade-dependent (parthenolide-induced) and cascade-independent (Taxol-induced) pathways, and the induction of NF-κB and its ability to promote resistance to apoptosis could be blocked by parthenolide.

Although adjuvant approaches targeting NF-κB in combination with Taxol have been reported for prostate cancer, pancreatic cancer, and breast cancer (3-9), there have been no reports investigating an adjuvant approach in combination with Taxol

for lung cancer, especially for *in vivo* models. In the present study, activation of NF-κB was significantly induced by Taxol in Taxol-resistant cancer cell lines, whereas Taxol-sensitive A549 cells do not have significant constitutive activation of NF-κB. This supports NF-κB activation as a cellular mechanism of apoptosis resistance, which is consistent with reports in ovarian cancer, prostate cancer, pancreatic cancer, and breast cancer. Our results also indicate that the phosphorylation level of IKKβ remarkably increases by Taxol, whereas p-IKKα is essentially not affected, which parallels NF-κB activation. Thus, it seems that constitutive activation of NF-κB mediates Taxol resistance in human NSCLC cells and inhibition of NF-κB activation sensitizes human NSCLC cells to Taxol.

Most studies of the inhibition of NF-κB activity have used a gene therapy approach. However, the advantage of soluble inhibitors is that their delivery would be easier and more efficient than gene transfer. Small molecules that inhibit IKK activity have indeed been described, and some of these molecules have been shown to induce apoptosis in cancer cells (19-21, 31-33). However, compounds that inhibit IKK with very high affinities have not been reported. Here, we describe the inhibition of IKK activity by a novel compound parthenolide that shows strong anticancer activity. We observed that the cytotoxic effect of Taxol was potentiated by pretreatment with 5 μmol/L parthenolide; at this concentration, we did not see a noticeable induction of apoptosis by parthenolide alone. Previous publications suggest

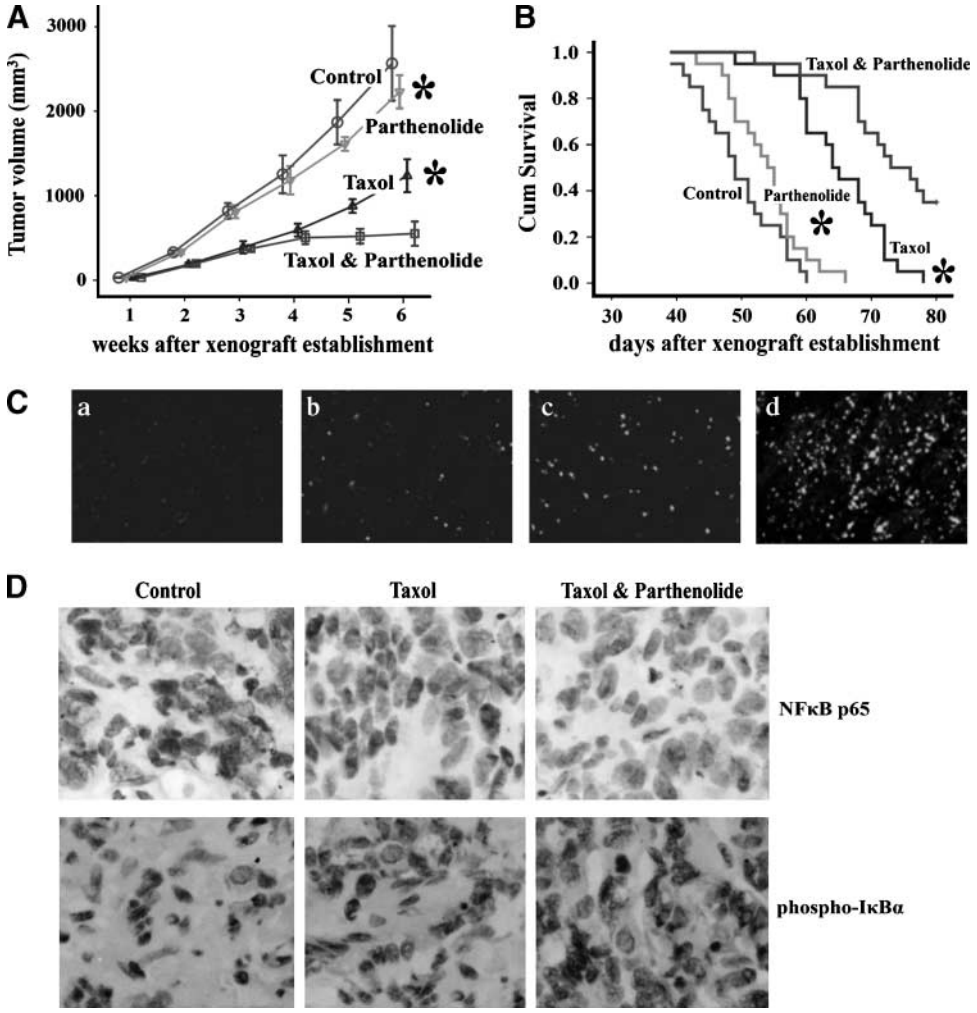

FIGURE 6. Potentiation of Taxol-induced cytotoxicity by parthenolide *in vivo*. **A.** Regression of A549 tumor xenografts in mice treated concurrently with Taxol and parthenolide. Human A549 tumor-bearing nude mice were established as described in the Materials and Methods. Drug treatment groups received Taxol, parthenolide, or Taxol and parthenolide. The tumor volumes were measured on the indicated day. *, $P < 0.01$ versus Taxol and parthenolide group. **B.** Kaplan-Meier curve showing survival in combined treatment mice compared with the controls. A significant increase in survival of Taxol and parthenolide group was observed. **C.** Induction of the apoptosis *in vivo*. After daily intratumoral injection of the indicated treatment (*a,* Control; *b,* Taxol; *c,* parthenolide; *d,* Taxol and parthenolide) for 6 wk, the xenografts were collected, sectioned, and stained for apoptotic cells by TUNEL, which were done as described in the Materials and Methods. Apoptotic nuclei (*green*) were identified by TUNEL staining with FITC-dUTP and observed under a fluorescence microscope (×200). **D.** I-κBα phosphorylation status and subcellular localization of NF-κB p65 were assessed by immunohistochemistry with anti–phospho-I-κBα antibody (**A**) and anti–NF-κB p65 antibody (**B**), respectively. Both nuclear and cytoplasmic staining patterns were observed, but the pattern was essentially nuclear with RelA/NF-κB staining and cytoplasmic with I-κBα staining. Representative pattern of increased RelA/NF-κB and phosphorylated I-κBα staining in both the cytoplasm and nuclei are shown (original magnification, ×400).

that pretreatment is a prerequisite to enhance cell sensitization to chemotherapy agents (34). Similarly, we found that pretreatment has a synergistic effect on Taxol cell sensitivity, but not on simultaneous treatment. *In vivo*, the Taxol/parthenolide combination induces tumor regression at doses that are well-tolerated in mice and is an attractive alternative to using high doses of single agents that may have significant cumulative toxicity. We did not detect significant renal, hepatic, or pulmonary tissue toxicity in this study. A previous study also showed that using up to 20 mg/kg/day of these agents in rats for 21 days did not cause obvious toxicity (21, 22). Combination treatment with Taxol and parthenolide is also associated with decreased angiogenesis, which may further enhance the efficacy observed *in vivo*. These findings validate the synergism of these drugs observed in cell lines growing in culture.

In contrast to aspirin, which selectively inhibits IKKβ but not IKKα (35), the IKK inhibitor, parthenolide, described here inhibits the activity of both IKKα and IKKβ. But whether Taxol-induced up-regulation and parthenolide-induced down-regulation of p65 are regulated only through IKKβ is neither clear from other studies or from ours. As indicated in some reports, Taxol could directly induce phosphorylation of I-κBα (21). Several other studies have also shown that Taxol could directly activate survival pathways such as Bcl-2, Akt, Cox-2, mitogen-activated protein kinase, etc., independently of NF-κB (36, 37). Transfection with an siRNA against IKKα and/or IKKβ could completely abolish parthenolide activity in this study, whereas the overexpression of IKKβ in cells could reverse the activity of parthenolide and showed significant Taxol resistance. This indicates that parthenolide might mediate the NF-κB/I-κB cascade mainly through IKKβ inhibition in this combination usage. Taken together, targeting IKK to inhibit NF-κB activity showed its potential use in combination with chemotherapeutic drugs involving in NF-κB signaling pathway.

On the basis of these observations, if the activation of NF-κB is the key mediator reversibly induced by parthenolide and Taxol, the question then becomes as follows: what is the possible downstream target of NF-κB that mediates the apoptosis signaling cascade? Recent studies have identified that activation of caspases and mitochondria seems to be a mere bystander effect of Taxol treatment of NSCLC cell lines (29, 38), whereas mitochondria cytochrome *c* release during NF-κB inhibition had been described previously. Hence, it would be interesting to examine whether the mitochondria participates in the mediation of Taxol-induced I-κBα degradation. Our results indicate that the mitochondria apoptotic route does not play an essential role in Taxol-induced cell death, as shown by the finding that inhibition of these pathways by Z-VAD-fmk resulted only in a temporary protection. This suggests the existence of an alternative, caspase-independent apoptotic mechanism for Taxol. Concomitant with synergistic toxicity, Taxol plus parthenolide, at a concentration of 5 μmol/L, induced caspase activation, which could blocked by caspase inhibitor zVAD-fmk, indicating the apoptotic effect of parthenolide is mainly through the caspase cascade and mitochondrial pathways. Treatment with Taxol plus parthenolide also increased cytochrome *c* release more than Taxol alone. Furthermore, the time course study showed that the level of phosphorylated I-κBα, which was also reduced by Taxol, was parallel to that of cytochrome *c* and could be blocked by an siRNA against IKKβ, indicating that cytochrome *c* and NF-κB may act in concert in response to the treatment. This result is also consistent with reports published previously with other systems (39, 40).

It was reported that NF-κB activation could result in transcription of some antiapoptotic genes, such as Bcl-xl (41-43), one of the antiapoptotic Bcl-2 family proteins responsible for mitochondrial membrane permeabilization. Our results showed that Bcl-xl protein was expressed at significantly higher levels in A549 cells induced with Taxol, whereas expression of Bcl-xl was reduced when cells were treated with parthenolide in combination with Taxol through down-regulation of NF-κB signaling, effects that paralleled their synergistic toxicity in A549 cancer cells. Overexpression of Bcl-2 family proteins could render cells resistant to apoptosis (43). Neutralization of Bcl-xl by siRNA depletion of the protein did not induce cell death by itself, but restored the apoptotic response to Taxol. These observations indicated that the combined effect of Taxol and parthenolide comes from decreased Bcl-xl induction, which could stabilize the mitochondrial membrane through the inhibition of NF-κB activity by parthenolide. These data support the idea that the synergistic cellular toxicity was at the level of NF-κB and downstream antiapoptotic factors. This is consistent with recent data that showed that a small-molecule inhibitor of Bcl-2 family proteins enhanced the apoptotic effects of chemotherapeutics and radiation in NSCLC (44).

Altogether, we showed that combination treatment with parthenolide and Taxol is significantly superior to Taxol or parthenolide alone and we further obtained important insights into the mechanism. Parthenolide, which could activate the IKK pathway and subsequent inhibit NF-κB and its downstream antiapoptotic proteins, was tested in the main human NSCLC cell lines. In addition, previous data support the hypothesis that combining mechanistically similar drugs, which share at least one target, is a viable strategy that can result in a greater than additive therapeutic benefit (45-48). Further studies are in progress in our laboratory to delineate the role of these proteins in the execution of the synergistic effect by Taxol and parthenolide. In this regard, parthenolide reported in this study may be useful in combination therapy with Taxol, with potential utility in treating refractory tumors and thus, conveying a survival benefit to cancer patients without the potential disadvantage of adverse side effects.

Materials and Methods

Drugs

Parthenolide was obtained from Alexis Biochemicals. Taxol was purchased from Calbiochem, and BAY 11-7082 and Z-VAD-fmk was purchased from Biomol (BIOMOL International L.P). These agents were dissolved in DMSO at a concentration of 10 or 20 mmol/L and stored in the dark at −80°C.

Cell Cultures

The cells, including human lung adenocarcinoma cell line A549 and squamous cell line NCI-H446, were obtained from the Cell Bank of the Chinese Academy of Sciences. A549 Taxol-resistant derivative A549-T24 was selected for resistance to

Taxol in a stepwise manner and maintained at a final concentration of 24 nmol/L of Taxol. Stable transfectants of A549 cells expressing IKKβ (49) were maintained at 37°C in a water-saturated atmosphere of 95% air and 5% CO_2, in tissue culture flasks containing RPMI 1640 (Life Technologies) supplemented with 10% (v/v) fetal bovine serum and 100 units/mL each of penicillin and streptomycin.

Small Interfering RNA

The high-purity SMARTpool siRNAs of IKKα, IKKβ, and control siRNA were purchased from Upstate. The lipid-encapsulated SMARTpool and control were used for transfection. At the time of transfection, cells were approximately 70% to 90% confluent, at a density of $\sim 1 \times 10^5$ cells/mL. We transfected the siRNAs into cells using the siIMPORTER Transfection Reagent (Upstate) following the manufacturer's protocol. Bcl-xl target sequence used was 5′-AGCAUAUCAGAGCUUUGAA-3′, and the siRNA duplexes were synthesized by Shanghai Sangon Biotech. A luciferase siRNA duplex (5′-CAUUCUAUCCUCUAGAGGAUG-3′) was used as a control. Transient transfection of siRNA duplexes was done using Lipofectamine 2000 (Invitrogen). The same siRNA reagents were added to the media for a second 24 h. Gene silencing effects were evaluated by Western blot analysis. At 24 h after transfection, cells were treated with Taxol as described above.

Cell Viability Determination [3-(4,5-dimethylthiazol-2-yl)-2,5-diphenyltetrazolium bromide Assay]

Cell proliferation was measured by a colorimetric assay. Aliquots (10 μL) of 3-(4,5-dimethylthiazol-2-yl)2,5-diphenyltetrazolium bromide solution (10 mg/mL in PBS) were used as the substrate, and 100 μL of 10% SDS was used to form formazan crystals. The absorption of the samples was determined using an ELISA reader (Anthos Mikrosysteme GmBH) at wavelength of 570 nm following the manufacturer's instructions.

Mitochondrial Membrane Permeabilization (Mitotracker) Assay

Mitochondrial integrity was determined by the mitochondrial fluorescence intensity of mitochondrial dye Mitotracker Red (Molecular Probes). Cells were exposed to different treatments in medium containing 0.5% fetal bovine serum for the indicated periods of time described above. The cells were incubated with 100 nmol/L dye for 45 min at 37°C under 5% CO_2. Cells were then collected, washed with PBS, and resuspended in PBS + 1% fetal bovine serum. The mitochondrial fluorescence intensity was quantified by fluorescence-activated cell sorting analysis (Calibur). All flow cytometry analyses were repeated thrice.

Nuclear Extracts and EMSA

Nuclear extracts and EMSA was done as described previously (10). Briefly, double-stranded oligonucleotide probes (NF-κB, 5′-AGT TGA GGG GAC TTT CCC AGG C-3′; Oct-1, 5′-ATGCAAAT-3′) were labeled with T4 polynucleotide kinase and γ-^{32}P ATP (Yahui Biotech, Inc.). Protein extract (10 μg) was incubated with 2×10^4 cpm of oligonucleotide probe along with 1 μg poly(deoxyinosinic-deoxycytidylic acid) (Sigma) in binding buffer for 15 min at room temperature. The resulting protein-DNA complexes were analyzed on 4% nondenaturing polyacrylamide gels in 0.5× Tris-borate-EDTA buffer and then subsequently dried and analyzed by autoradiography. Equal loading of nuclear extracts was monitored by Oct-1 binding.

Western Blot Analysis

Following drug treatment, attached and floating cells were collected and lysed using protein extraction buffer, then homogenized in 250 μL of lysis buffer. Cytoplasmic extracts (10 μg of total protein) were electrophoresed on 4% to 20% gradient SDS-PAGE gels (Shanghai Sangon Biotech) and transferred to nylon membranes (Shanghai Sangon Biotech). Blots were probed with various specific primary antibodies to recognize their respective proteins. The secondary antibody, horseradish peroxidase–coupled mouse anti-rabbit immunoglobulin (Jingmei Biotech Co., Ltd.), was subsequently incubated for 1 h at room temperature. The subsequent analysis of protein was done with chemiluminescence using an enhanced chemiluminescence Western blotting kit (Amersham Biosciences) following the manufacturer's recommendations.

Immunofluorescence Assays

For immunostaining, the cells were fixed and stained with primary antibodies including anti–NF-κB (p65; 1:200; Santa Cruz Biotechnology, Inc.) or anti- cytochrome *c* (1:200; #4272, Cell Signaling Technology). The cells were then incubated with affinity-purified, rhodamine-conjugated mouse anti-rabbit IgG (1:4000; Jackson Immuno Research). The stained cells were analyzed under a fluorescence microscopy confocal microscope (Leica Microsystems Heidelberg GmbH) with excitation at 488 nm and emission at 525 nm.

Cytochrome c Release Assay

Cytochrome *c* release was assayed with the Cytochrome *c* Apoptosis Assay kit (Biovision). Briefly, cells were homogenized with the cytosol extraction buffer provided in the kit and then centrifuged to remove the debris. The supernatant was collected as the cytosolic fraction. These fractions were analyzed for cytochrome *c* by Western blot using the cytochrome *c* antibody provided.

Animal Tumor Models and Treatment

All of the procedures involving animals and their care in this study were approved by the institute's Animal Care and Use Committee of Chongqing Medical University. Human A549 tumor models were established in 6- to 8-wk-old, athymic nude mice (SPF grade), which were obtained from Chongqing Medical University Animal Center. Athymic nude mice were inoculated with A549 cells/0.1 mL (1.0×10^7) s.c. on the left side of the armpit. Two weeks after inoculation, the animals were randomly divided into four groups (eight animals/group) and received one of the following treatments by a single i.p. injection into the lower right quadrant of the peritoneum: one group of mice ($n = 6$) was treated with parthenolide (5 mg/kg) thrice weekly plus Taxol (5 mg/kg) weekly for 4 wk. A second group of mice ($n = 6$) was treated with parthenolide alone (5 mg/kg) thrice weekly for 4 wk. A third group ($n = 6$) was treated with Taxol alone (5 mg/kg) weekly for 4 wk. The control group ($n = 6$) received vehicle (PBS) alone. Tumor size and body weight were measured twice weekly. Tumor size was determined by caliper measurement of the largest and perpendicular diameters. Tumor volume was calculated according to the

formula $V = 0.52ab^2$. At the end of the experiment, mice underwent euthanasia with CO_2. The tumor tissue was excised, fixed, and embedded in paraffin for histochemical analysis.

Immunohistochemistry

Immunohistochemistry was carried out in paraffin-embedded (5 μm) tissue sections. Assessment of apoptosis was done as reported previously by TUNEL staining using an *in situ* cell death detection kit (Roche Molecular Biochemicals) according to the manufacturer's protocol. For analysis of expression of phospho-IκBα and localization of NF-κB p65, slides were incubated with anti-RelA against the p65 (RelA) unit (p65; 1:150; sc-109; Santa Cruz Biotechnology), anti-phosphorylated IκBα that recognizes the epitope Ser 32 (1:40; sc-8404; Santa Cruz Biotechnology), anti-IκBα (1:100; sc-1643; Santa Cruz Biotechnology), and incubated with secondary antibodies (goat anti-mouse immunoglobulins; Shanghai Sangon Biotech). Five equal-sized fields were randomly chosen and analyzed.

Statistical Analysis

Statistical analysis was carried out using one-way ANOVA followed by Fisher's least significant difference test, and the level of significance was set at a P value of <0.05. Data are expressed as the mean ± SE. Survival curves were constructed using the Kaplan-Meier method and compared using the log-rank test. Statistical comparisons were carried out using SPSS software for Windows (SPSS, Inc.).

Disclosure of Potential Conflicts of Interest

No potential conflicts of interest were disclosed.

Acknowledgments

We thank Prof. Wang Wei for providing technical assistance and insightful discussions during the preparation of the manuscript. We thank Dr. Xiaoyong Zhang at the Wistar Institute for help with the linguistic revision of the manuscript.

References

1. Riedel RF, Porrello A, Pontzer E, et al. A genomic approach to identify molecular pathways associated with chemotherapy resistance. Mol Cancer Ther 2008;7:3141–9.

2. Ni J, Takayama K, Ushijima R, et al. Adenovirus-mediated inhibitor κB gene transfer improves the chemosensitivity to anticancer drugs in human lung cancer *in vitro* and *in vivo*. Anticancer Res 2008;28:601–8.

3. Mabuchi S, Ohmichi M, Nishio Y, et al. Inhibition of inhibitor of nuclear factor-κB phosphorylation increases the efficacy of taxol in *in vitro* and *in vivo* ovarian cancer models. Clin Cancer Res 2004;10:7645–54.

4. Kimura A, Ohmichi M, Kawagoe J, et al. Induction of hTERT expression and phosphorylation by estrogen via Akt cascade in human ovarian cancer cell lines. Oncogene 2004;23:4505–15.

5. Mabuchi S, Ohmichi M, Nishio Y, et al. Inhibition of NFκB increases the efficacy of cisplatin in *in vitro* and *in vivo* ovarian cancer models. J Biol Chem 2004;279:23477–85.

6. Fujioka S, Sclabas GM, Schmidt C, et al. Function of nuclear factor κB in pancreatic cancer metastasis. Clin Cancer Res 2003;9:346–54.

7. Montagut C, Tusquets I, Ferrer B, et al. Activation of nuclear factor-κB is linked to resistance to neoadjuvant chemotherapy in breast cancer patients. Endocr Relat Cancer 2006;13:607–16.

8. Wang Q, Yang W, Uytingco MS, Christakos S, Wieder R. 1,25-Dihydroxyvitamin D3 and all- *trans*-retinoic acid sensitize breast cancer cells to chemotherapy-induced cell death. Cancer Res 2000;60:2040–8.

9. Fradet V, Lessard L, Bégin LR, Karakiewicz P, Masson AM, Saad F. Nuclear factor-κB nuclear localization is predictive of biochemical recurrence in patients with positive margin prostate cancer. Clin Cancer Res 2004;10:8460–4.

10. Zhang D, Jin X, Wang F, et al. Combined prognostic value of both RelA and IκB-α expression in human non-small cell lung cancer. Ann Surg Oncol 2007;14:3581–92.

11. Stathopoulos GT, Sherrill TP, Cheng DS, et al. Epithelial NF-{κ}B activation promotes urethane-induced lung carcinogenesis. Proc Natl Acad Sci U S A 2007;104:18514–9.

12. Tang X, Liu D, Shishodia S, et al. Nuclear factor-κB (NF-κB) is frequently expressed in lung cancer and preneoplastic lesions. Cancer 2006;107:2637–46.

13. Dong QG, Sclabas GM, Fujioka S, et al. The function of multiple IκB: NF-κB complexes in the resistance of cancer cells to Taxol-induced apoptosis. Oncogene 2002;21:6510–9.

14. Pahl HL. Activators and target genes of Rel/NF-κB transcription factors. Oncogene 1999;18:6853–66.

15. Wang J, An H, Mayo MW, Baldwin AS, Yarbrough WG. LZAP, a putative tumor suppressor, selectively inhibits NF-κB. Cancer Cell 2007;12:239–51.

16. Bassères DS, Baldwin AS. Nuclear factor-κB and inhibitor of κB kinase pathways in oncogenic initiation and progression. Oncogene 2006;25:6817–30.

17. Loercher A, Lee TL, Ricker JL, et al. Nuclear factor-κB is an important modulator of the altered gene expression profile and malignant phenotype in squamous cell carcinoma. Cancer Res 2004;64:6511–23.

18. Oyaizu H, Adachi Y, Okumura T, et al. Proteasome inhibitor 1 enhances taxol-induced apoptosis in human lung adenocarcinoma cell line. Oncol Rep 2001;8:825–9.

19. Yang J, Amiri KI, Burke JR, Schmid JA, Richmond A. BMS-345541 targets inhibitor of κB kinase and induces apoptosis in melanoma: involvement of nuclear factor κB and mitochondria pathways. Clin Cancer Res 2006;12:950–60.

20. Saadane A, Masters S, DiDonato J, Li J, Berger M. Parthenolide inhibits IκB kinase, NF-κB activation, and inflammatory response in cystic fibrosis cells and mice. Am J Respir Cell Mol Biol 2007;36:728–36.

21. Bava SV, Puliappadamba VT, Deepti A, Nair A, Karunagaran D, Anto RJ. Sensitization of taxol-induced apoptosis by curcumin involves down-regulation of nuclear factor-κB and the serine/threonine kinase Akt and is independent of tubulin polymerization. J Biol Chem 2005;280:6301–8.

22. Oka D, Nishimura K, Shiba M, et al. Sesquiterpene lactone parthenolide suppresses tumor growth in a xenograft model of renal cell carcinoma by inhibiting the activation of NF-κB. Int J Cancer 2007;120:2576–81.

23. Kishida Y, Yoshikawa H, Myoui A. Parthenolide, a natural inhibitor of Nuclear Factor-κB, inhibits lung colonization of murine osteosarcoma cells. Clin Cancer Res 2007;13:59–67.

24. Patel NM, Nozaki S, Shortle NH, et al. Taxol sensitivity of breast cancer cells with constitutively active NF-κB is enhanced by IκBα super-repressor and parthenolide. Oncogene 2000;19:4159–69.

25. Yip-Schneider MT, Nakshatri H, Sweeney CJ, Marshall MS, Wiebke EA, Schmidt CM. Parthenolide and sulindac cooperate to mediate growth suppression and inhibit the nuclear factor-κ B pathway in pancreatic carcinoma cells. Mol Cancer Ther 2005;4:587–94.

26. Yip-Schneider MT, Wu H, Ralstin M, Yiannoutsos C, et al. Suppression of pancreatic tumor growth by combination chemotherapy with sulindac and LC-1 is associated with cyclin D1 inhibition *in vivo*. Mol Cancer Ther 2007;6:1736–44.

27. Ralstin MC, Gage EA, Yip-Schneider MT, Klein PJ, Wiebke EA, Schmidt CM. Parthenolide cooperates with NS398 to inhibit growth of human hepatocellular carcinoma cells through effects on apoptosis and G0–1 cell cycle arrest. Mol Cancer Res 2006;4:387–99.

28. Park SJ, Wu CH, Gordon JD, Zhong X, Emami A, Safa AR. Taxol induces caspase-10-dependent apoptosis. J Biol Chem 2004;279:51057–67.

29. Huisman C, Ferreira CG, Bröker LE, et al. Taxol triggers cell death primarily via caspase-independent routes in the non-small cell lung cancer cell line NCI-H460. Clin Cancer Res 2002;8:596–606.

30. Jones DR, Broad RM, Comeau LD, Parsons SJ, Mayo MW. Inhibition of nuclear factor κB chemosensitizes non-small cell lung cancer through cytochrome *c* release and caspase activation. J Thorac Cardiovasc Surg 2002;123:310–7.

31. Holmes-McNary M, Baldwin AS, Jr. Chemopreventive properties of *trans*-resveratrol are associated with inhibition of activation of the IκB kinase. Cancer Res 2000;60:3477–83.

32. Vivat-Hannah V, You D, Rizzo C, et al. Synergistic cytotoxicity exhibited by combination treatment of selective retinoid ligands with taxol (Taxol). Cancer Res 2001;61:8703–11.

33. Liu X, Yue P, Chen S, et al. The proteasome inhibitor PS-341 (bortezomib) up-regulates DR5 expression leading to induction of apoptosis and enhancement of TRAIL-induced apoptosis despite up-regulation of c-FLIP and survivin expression in human NSCLC cells. Cancer Res 2007;67:4981–8.

34. Bava SV, Puliappadamba VT, Deepti A, Nair A, Karunagaran D, Anto RJ. Sensitization of taxol-induced apoptosis by curcumin involves down-regulation of nuclear factor-κB and the serine/threonine kinase Akt and is independent of tubulin polymerization. J Biol Chem 2005;280:6301–8.

35. Yin MJ, Yamamoto Y, Gaynor RB. The anti-inflammatory agents aspirin and salicylate inhibit the activity of I(κ)B kinase-β. Nature 1998;396:77–80.

36. Mabuchi S, Ohmichi M, Kimura A, et al. Inhibition of phosphorylation of BAD and Raf-1 by Akt sensitizes human ovarian cancer cells to taxol. J Biol Chem 2002;277:33490–500.

37. Subbaramaiah K, Hart JC, Norton L, Dannenberg AJ. Microtubule-interfering agents stimulate the transcription of cyclooxygenase-2. Evidence for involvement of ERK1/2 AND p38 mitogen-activated protein kinase pathways. J Biol Chem 2000;275:14838–45.

38. Bröker LE, Kruyt FA, Giaccone G. Cell death independent of caspases: a review. Clin Cancer Res 2005;11:3155–62.

39. Okano J, Rustgi AK. Taxol induces prolonged activation of the Ras/MEK/ERK pathway independently of activating the programmed cell death machinery. J Biol Chem 2001;276:19555–64.

40. Ling Y, Zhong Y, Perez-Soler R. Disruption of cell adhesion and caspase-mediated proteolysis of β- and γ-catenins and APC protein in taxol-induced apoptosis. Mol Pharmacol 2001;59:593–603.

41. Farhana L, Dawson MI, Fontana JA. Apoptosis induction by a novel retinoid-related molecule requires nuclear factor-κB activation. Cancer Res 2005;65:4909–17.

42. Dolcet X, Llobet D, Encinas M, et al. Proteasome inhibitors induce death but activate NF-κB on endometrial carcinoma cell lines and primary culture explants. J Biol Chem 2006;281:22118–30.

43. Kim SH, Hwang CI, Juhnn YS, Lee JH, Park WY, Song YS. GADD153 mediates celecoxib-induced apoptosis in cervical cancer cells. Carcinogenesis 2007;28:223–31.

44. Oltersdorf T, Elmore SW, Shoemaker AR, et al. An inhibitor of Bcl-2 family proteins induces regression of solid tumours. Nature 2005;435:677–81.

45. Dy GK, Thomas JP, Wilding G, et al. A phase I and pharmacologic trial of two schedules of the proteasome inhibitor, PS-341 (bortezomib, velcade), in patients with advanced cancer. Clin Cancer Res 2005;11:3410–6.

46. Horton TM, Pati D, Plon SE, et al. A phase 1 study of the proteasome inhibitor bortezomib in pediatric patients with refractory leukemia: a Children's Oncology Group study. Clin Cancer Res 2007;13:1516–22.

47. Nakshatri H, Rice SE, Bhat-Nakshatri P. Antitumor agent parthenolide reverses resistance of breast cancer cells to tumor necrosis factor-related apoptosis-inducing ligand through sustained activation of c-Jun N-terminal kinase. Oncogene 2004;23:7330–44.

48. Karin M, Yamamoto Y, Wang QM. The IKK NF-κB system: a treasure trove for drug development. Nat Rev Drug Discov 2004;3:17–26.